



Contents lists available at ScienceDirect

Arabian Journal of Chemistry

journal homepage: www.sciencedirect.com



Original article

Estimation of vanadium removal from calcification roasting-acid leaching tailings using ultrasonic-H₂C₂O₄ synergistic technology

Haoyu Li ^{a,*}, Qian Ren ^a, Shihong Tian ^b, Jun Wang ^{a,**}, Xuejun Zhu ^a, Tao Yang ^a, Yi Zhang ^a, Jingjing Liu ^c, Jiayuan Liu ^d

^a College of Biological and Chemical Engineering (College of Agricultural Sciences), Panzhihua University, Panzhihua 617000, China

^b Chongqing Institute of Green and Intelligent Technology, Chinese Academy of Sciences, Chongqing 400714, China

^c College of Vanadium and Titanium, Panzhihua University, Panzhihua 617000, China

^d Sichuan Metallurgical Geological Exploration Bureau 601 Brigade, Panzhihua 617000, China



ARTICLE INFO

Article history:

Received 7 July 2023

Accepted 7 October 2023

Available online 11 October 2023

Keywords:

Vanadium tailings

Ultrasonic

Oxalic acid

Synergistic technology

Cleaner production

ABSTRACT

Metal vanadium smelting produces roasting-acid leaching tailings containing approximately 1% vanadium residue, making it challenging to store and recycle these waste tailings in an environmentally friendly manner. To address this issue, a clean method called ultrasonic-enhanced oxalic acid complexation was proposed in this study for efficient removal of residual vanadium. Under the optimal conditions, the removal rate of vanadium and the decomposition rate of oxalic acid reached 86.88% and 23.6%. An in-depth analysis on the experimental results in combination with thermodynamics found a virtuous cycle chain induced by ultrasonic cavitation. Ultrasonic waves facilitated the decomposition of oxalic acid, producing more CO₂ to supplement the limited cavitation bubble nucleuses. Consequently, the cavitation effect was strengthened, leading to an increased yield of OH radicals. This resulted in a continuous improvement in the oxidation environment. Furthermore, the enhanced virtuous cycle generated by ultrasonic cavitation produced powerful microjets that facilitated the stripping and dispersion of mineral particles. Overall, the oxalic acid-ultrasonic leaching technique offers a clean and efficient technology for separating vanadium.

© 2023 The Author(s). Published by Elsevier B.V. on behalf of King Saud University. This is an open access article under the CC BY-NC-ND license (<http://creativecommons.org/licenses/by-nc-nd/4.0/>).

1. Introduction

Vanadium, an indispensable strategic metal, finds extensive applications in various industries such as aerospace, energy storage, metallurgy, and special ceramics. One of its significant uses is in the preparation of vanadium batteries, which plays a crucial role in the advancement of energy storage systems (Liu et al., 2023). With the continuous development of the vanadium smelting industry, large amounts of calcification roasting-acid leaching (CRAL) tailings have been produced worldwide (Wang et al.,

2023; Wang et al., 2022). Although CRAL tailings have been used commercially to prepare vanadium-titanium porcelain, far-infrared coating, and slagging agent, their consumption remains limited due to low utilization rates (Li et al., 2020). Traditionally, CRAL tailings are often accumulated in tailings ponds during the treatment process. However, both storage and recycling of waste residues must adhere to production safety requirements while complying with national standards to prevent re-pollution (Opferkuch et al., 2021). Cheng et al. found that the high vanadium content (about 1%) in CRAL tailings results in leaching toxicity (Cheng et al., 2023). During piling processes, rainfall can cause vanadium to penetrate into soil and groundwater systems, leading to extensive environmental pollution that poses a threat to ecosystems (Petranikova et al., 2020). The elevated levels of residual vanadium can be attributed to two main factors. Firstly, certain low-valence V species, such as V(III) and V(IV), within refractory phases like spinel and gangue, are not fully oxidized to V(V) during industrial production, thus remaining un-leached in the solutions. Secondly, there is an obvious limitation on using H₂SO₄ as a leaching agent in conventional processes (Hu et al., 2023). The

* Corresponding author.

** Corresponding author.

E-mail addresses: 18213836872@163.com (H. Li), enjoygreenlife@126.com (J. Wang).

Peer review under responsibility of King Saud University.



Production and hosting by Elsevier

introduction of SO_4^{2-} leads to the formation of CaSO_4 colloid which may prevent the contact between the leaching system and vanadium, thereby reducing efficiency. Therefore, it is crucial to find a clean and efficient method for releasing and oxidizing low-valence vanadium by effectively destroying these inclusions, ensuring sustainable development within the vanadium industry.

Studies have shown that there are several techniques available for separating and extracting vanadium from minerals, including roasting leaching, direct leaching, biological leaching, and molten salt electrolysis (Peng, 2019; Liu et al., 2021a; Guo et al., 2023; Li et al., 2023). However, the most commonly used method in industry involves the use of strong acids, such as sulfuric acid, for non-differential leaching of metal elements. Unfortunately, the utilization rate of sulfuric acid is low, and its wastewater treatment poses challenges. Moreover, the corrosion caused by sulfuric acid on equipment can significantly increase production costs and have negative economic implications (Liu et al., 2021b). To address these issues, researchers have been exploring alternative leaching agents, and one promising candidate is oxalic acid. Oxalic acid, a low molecular weight organic acid, has a strong coordination effect and has been found to effectively dissolve minerals (Li et al., 2021). Experimental results from Ma et al. (2023) suggest that oxalic acid may enhance the dissolution and migration of rare earth minerals, with higher concentrations demonstrating greater dissolution abilities. Furthermore, Rouquette et al. (2023) have proved the synergistic effect between H^+ and $\text{HC}_2\text{O}_4^-/\text{C}_2\text{O}_4^{2-}$. First, the H^+ provided by oxalic acid dissolves metal elements into a solution, and then, HC_2O_4^- and $\text{C}_2\text{O}_4^{2-}$ react with metal ions to form complex precipitation, thus completing the separation. In comparison to weak organic acids like malic acid, citric acid, and tartaric acid, which have high selectivity for target elements, oxalic acid stands out due to its ability to effectively dissolve the target element without the need for additional oxidizers to promote leaching efficiency. To determine the optimal acidity for organic acids, the acidity levels of commonly used complexing agents in the metallurgical industry were summarized (John, 2006), as shown in Table 1. Oxalic acid, one of the most acidic organic acids, can significantly enhance the acidity of the leaching environment, enabling fast complexation of $\text{C}_2\text{O}_4^{2-}$ with the target element. If the leaching system of oxalic acid demonstrates similar oxidation and mineral dissociation capabilities to sulfuric acid, it has the potential to replace inorganic acids as the preferred industrial leaching agent.

In the metallurgical industry, field intensification technology is widely utilized. Among these technologies, ultrasonic waves have been proven to have a significant impact in the recovery of various metals due to their cavitation effect, mechanical effect, and thermal effect. Researchers have explored the combination of ultrasonic irradiation with additives, organic acids, and other methods, which has shown great potential in enhancing metal leaching efficiency. For instance, Esmaeili et al. successfully recovered 100% nickel from waste Li-ion batteries by utilizing ultrasonic assistance with citric acid and H_2O_2 . It was found that the coexis-

tence of citric acid and H_2O_2 is a necessary condition for improving the ultrasonic leaching efficiency. Another example from He et al. involved the proposal of a new synergistic leaching system that combines mechanical activation with ultrasonic irradiation to extract zinc from ZnO ore. The results demonstrated a significant improvement in the zinc recovery rate under the synergistic effect of mechanical activation and ultrasonic irradiation. Compared to conventional leaching methods, this coupling leaching process not only enhances the leaching efficiency of zinc but also reduces the leaching time. Chen et al. made a groundbreaking introduction of ultrasonic technology into the process of leaching vanadium from low-grade vanadium-bearing shale. With the aid of ultrasound, the leaching efficiency of vanadium in an H_2SO_4 - CaF_2 medium was increased from 87.86% to 92.93%, and the leaching time was reduced from 240 min to 30 min. The combination of ultrasound and CaF_2 exhibited a more positive effect compared to ultrasound alone or the addition of CaF_2 , indicating a synergistic effect between ultrasound and CaF_2 . To summarize, the synergistic effect induced by ultrasonic waves has several benefits in metal recovery processes. It reduces the activation energy, accelerates the reaction speed, lowers the leaching temperature, and reduces the dosage of leaching agents. Therefore, the incorporation of ultrasound technology is likely to position oxalic acid as the preferred choice for industrial leaching agents.

Although ultrasonic technology has found widespread application in the metallurgical industry, the synergistic removal of vanadium from CRAL tailings when combined with oxalic acid remains unexplored. This study aims to assess the effects of oxalic acid concentration, reaction temperature, and ultrasonic intensity on both vanadium removal rate and oxalic acid consumption rate, with a focus on improving production efficiency and minimizing environmental impact. Thermodynamic calculations using FactSage 8.1 software were performed to identify bottlenecks in the wet treatment process. Additionally, mineral phase transformation analysis was conducted to elucidate the mechanism of ultrasonic enhancement in the oxidation reaction. The findings presented in this paper hold great significance for the comprehensive utilization of resources and the reduction of pollution from industrial waste.

2. Materials and methods

2.1. Materials

In this experiment, the CRAL tailings used for testing purposes were obtained from a local iron and steel plant located in Panzhihua, China. The CRAL tailings were initially in block-shaped form and underwent a series of processes including crushing, screening, and packaging. The resulting experimental raw tailings were obtained through the use of a 200 mesh screen. Table 2 provides the composition analysis of the main elements and vanadium content in these samples. The primary constituents of the tailings were determined to be iron (Fe) and manganese (Mn), with respective

Table 1
Dissociation constants of organic acids in aqueous solution (25 °C).

No.	Name	Chemical formula	K_a	$\text{p}K_a$
1	Oxalic acid	$(\text{COOH})_2$	$5.4 \times 10^{-2} (K_1)$	1.27
			$5.4 \times 10^{-5} (K_2)$	4.27
2	Glutamic acid	$\text{HOCOC}_2\text{H}_2\text{CH}(\text{NH}_2)\text{COOH}$	$7.4 \times 10^{-3} (K_1)$	2.13
			$4.9 \times 10^{-5} (K_2)$	4.31
			$4.4 \times 10^{-10} (K_3)$	9.36
3	Formic acid	HCOOH	1.8×10^{-4}	3.75
4	Glycolic acid	$\text{CH}_2(\text{OH})\text{COOH}$	1.48×10^{-4}	3.83
5	Lactic acid	$\text{CH}_3\text{CHOHCOOH}$	1.4×10^{-4}	3.86
6	Acetic acid	CH_3COOH	1.74×10^{-5}	4.76
7	Propionic acid	$\text{CH}_3\text{CH}_2\text{COOH}$	1.35×10^{-5}	4.87

Table 2
Main chemical elements in raw tailings.

Element	Fe	Mn	Cr	Ca	Ti	Si	S	V
Content (wt%)	37.93	15.00	11.54	9.36	9.27	7.33	6.00	0.84

content percentages of 37.93 wt% and 15.00 wt%. Other impurity elements present in the tailings mainly included chromium (Cr), calcium (Ca), titanium (Ti), silicon (Si), and sulfur (S). The vanadium ore grade in the raw tailings was measured at 0.84 wt%, slightly higher than the industrial mining requirement (Lee et al., 2021). Vanadium-bearing converter tailings typically comprise several components such as V_2O_5 , FeO , SiO_2 , TiO_2 , Cr_2O_3 , CaO , MgO , etc., making them a representative polymetallic co-producing resource. The X-ray diffraction (XRD) diagram, as shown in Fig. 1, confirmed that hematite, gypsum, mangano, chromite, ilmenite, and cristobalite were the main components of the raw tailings, presenting distinct vanadium-bearing converter tailings characteristics. Additionally, the scanning electron microscopy with energy-dispersive X-ray spectroscopy (SEM-EDS) characterization diagram in Fig. 2 revealed the presence of high oxygen content in the tailings, indirectly indicating the oxidizing characteristics of all the phases investigated. The element content analysis results at points 1 and 4 revealed that the vanadium content in $MnCr_2O_4$, Fe_2O_3 , and $Fe(TiO_3)$ (which can be expressed as $FeO \cdot TiO_2$) was lower than or equal to that in raw tailings. However, this was not the focus of this study. The element content analysis results at points 2 and 3 revealed that the vanadium content in $Ca(SO_4)(H_2O)_2$ and SiO_2 was about 2–10 times that in raw tailings, which formed the basis of the research attention during the leaching process.

X-ray photoelectron spectroscopy (XPS) was used to detect the different valence states and components of certain elements in the raw materials. The results, as shown in Fig. 3, indicated that the binding energy of $Fe2p$ exhibited two characteristic peaks at around 725 eV and 710 eV, which were identified as $Fe2p_{1/2}$ and

$Fe2p_{3/2}$, respectively, according to Verma et al. (2021). Further analysis utilizing Advantage software revealed eight peaks corresponding to Fe^{2+} and Fe^{3+} at 733.15 eV, 728.13 eV, 726.04 eV, 724.01 eV ($Fe2p_{1/2}$), 719.72 eV, 716.87 eV, 713.47 eV, and 711.03 eV ($Fe2p_{3/2}$), respectively. These findings were in agreement with the semi-quantitative analysis of Fe^{2+} and Fe^{3+} in the tailings was performed, which were found to be consistent with the results obtained from XRD analysis. The two characteristic peaks of $V2p$ at 525 eV and 517 eV corresponded to $V2p_{1/2}$ and $V2p_{3/2}$, respectively, which was consistent with the research results of Wang et al. (2013). Further analysis identified four peaks related to V^{4+} and V^{5+} at 524.88 eV, 523.63 eV, 517.41 eV, and 516.44 eV, respectively. This indicates that the majority of vanadium in the raw tailings existed in the $V(V)$ valence state, with a small fraction present as $V(IV)$. It was also found that some $V(IV)$ replaced $Al(III)$ in mica minerals through isomorphism. The replacement resulted in a stable mica structure, making it difficult to extract $V(IV)$ (Zhang et al., 2011). Therefore, the destruction of the vanadium-bearing mica lattice structure holds significant importance in facilitating vanadium extraction.

The experimental procedure involved the utilization of analytical grade chemical reagents, including oxalic acid, obtained from Sinopharm Chemical Reagent Co., Ltd., with a purity greater than 98%. To ensure the purity of the solutions, all aqueous solutions were prepared using distilled water.

2.2. Experimental procedure

In the leaching experiment, the objective was to determine the leaching efficiency of vanadium and iron from the raw tailings after

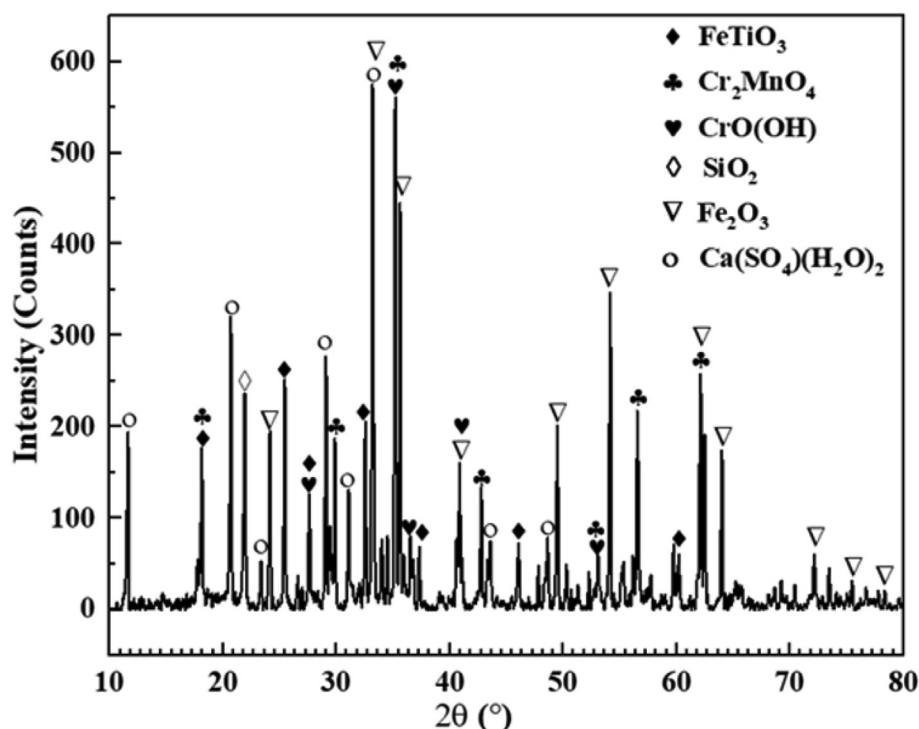


Fig. 1. X-ray pattern of the raw tailings.

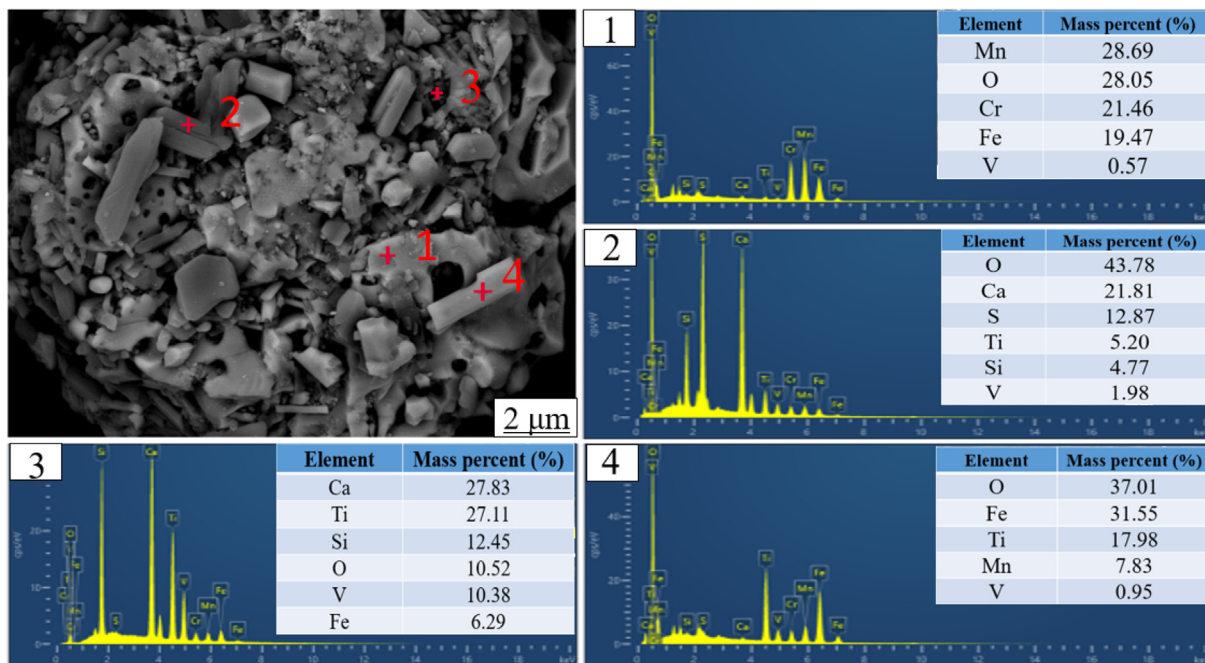


Fig. 2. SEM-EDS diagram of raw tailings.

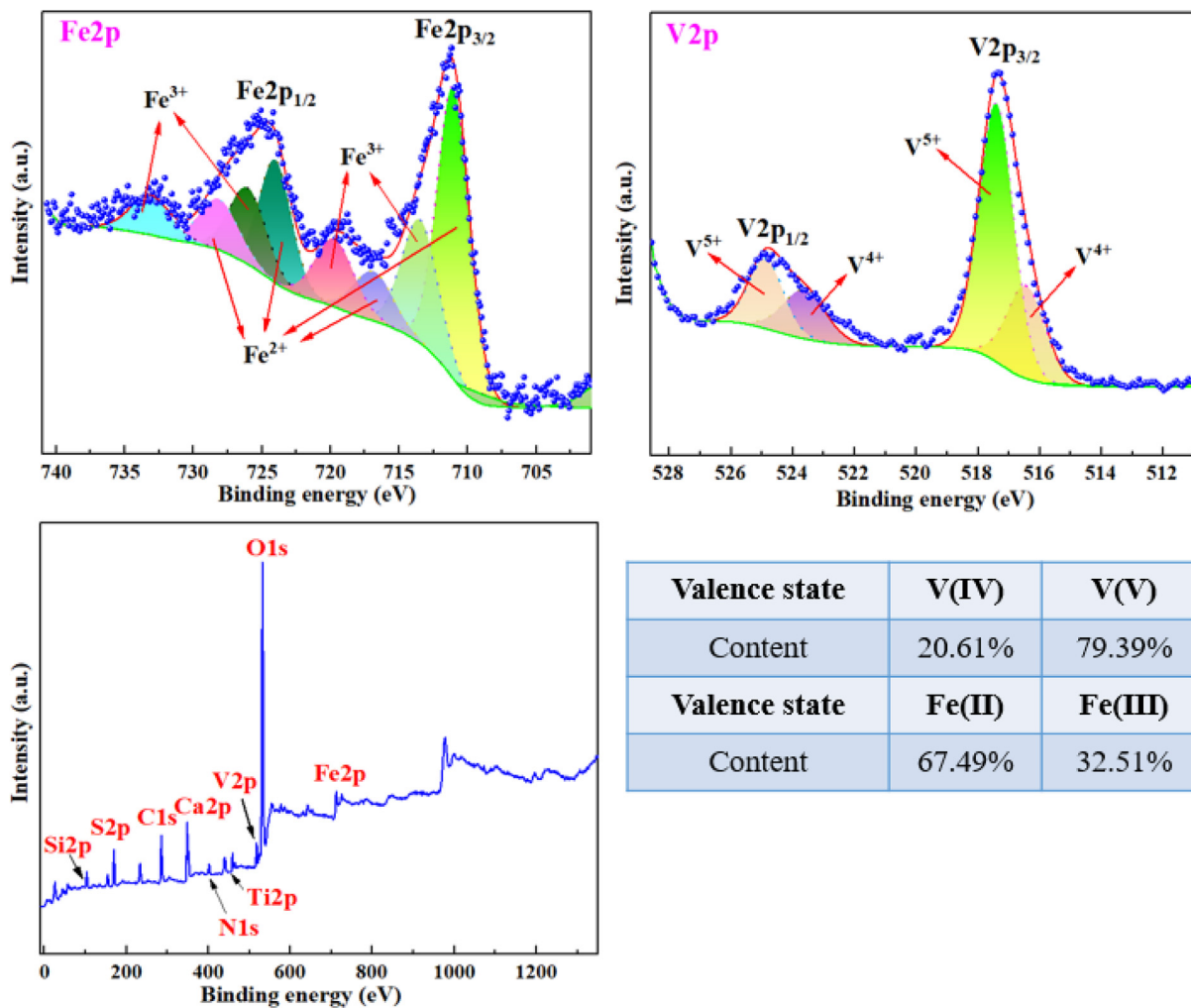


Fig. 3. XPS spectra of raw materials and the distribution of Fe and V contents in each valence state.

pretreatment. The raw tailings served as the starting material, while an oxalic acid solution with a specific concentration was used as the leaching agent. To control the experimental conditions, a constant temperature water bath kettle and electromagnetic stirring device were employed to regulate the temperature and rotational speed, respectively. The experimental setup involved placing a three-mouth beaker filled with the leaching agent into the constant temperature water bath kettle and initiating the stirring process. The temperature was gradually increased to the desired preset temperature, and the subsequent treatment was conducted at a constant temperature. The raw tailings were then added to the beaker, followed by ultrasonic treatment with a specified duration. After the leaching process, the solid and liquid components were separated, and the concentration of vanadium and iron in the dried leaching residues was determined. To evaluate the leaching efficiency, the leaching efficiency was calculated using the leaching formula represented by Formula (1)

$$\eta_V = \left(1 - \frac{m_2 \times \omega_{V2}}{m_1 \times \omega_{V1}} \right) \times 100\% \quad (1)$$

where, η_V represents the leaching efficiency of V; m_1 represents the mass of raw tailings (g); ω_{V1} represents the content of V in raw tailings (%); m_2 represents the mass of leaching residues (g); ω_{V2} represents the content of vanadium in leaching residues (%). The flow chart of the ultrasonic enhanced leaching experiment is shown in Fig. 4.

To validate the progress of the new process, a conventional acid leaching experiment was conducted under identical conditions as a reference blank experiment. Additionally, the variation in oxalic acid content was examined under both experimental conditions, namely conventional leaching and ultrasonic leaching, in the blank experiment without raw tailings. This analysis aimed to elucidate the synergistic effect of ultrasound and oxalic acid. The obtained results provided theoretical backing for the viability of this innova-

tive process. All experiments were replicated three times, and the average results were considered. To differentiate the two processes, the concept of differentials was introduced to calculate the specific distinctions between ultrasonic leaching and the conventional method. conventional leaching.

2.3. Characterizations

(1) Element content analysis

In this experiment, inductively coupled plasma optical emission spectroscopy (ICP-OES) was used to analyze the vanadium content in these samples (Mohanty et al., 2021). The solid sample was dissolved completely by the acid melting method and then transferred to a volumetric flask for preservation. In order to ensure the accuracy of the measurement structure, these samples were diluted to the standard concentration range for ICP measurement. The content of $H_2C_2O_4$ was measured by acid-base titration (Arif et al., 2023). The experiment was performed in triplicate. Finally, the content of $H_2C_2O_4$ was calculated as per the average value of three measurements.

(2) Component analysis

In the experiment, an X-ray fluorescence (XRF) spectrometer was used to analyze the chemical constituents of solid samples. When the sample was prepared, boric acid was used as the adhesion agent and pressed for 30 s under 40Mpa. Besides, the SST-mAX light tube and Hi-Per scintillation detector were adopted to perform quantitative analyses of O to U elements.

An X-ray diffractometer (XRD) was used to analyze the phase constituents of solid samples. Cu was selected as the XRD target material. The Cu target emitted the Ka line with a wavelength of 1.5419Å. The tube current was 40 mA and the tube voltage was 40 kV. The scanning range (2θ) was 10–90°. The scanning speed

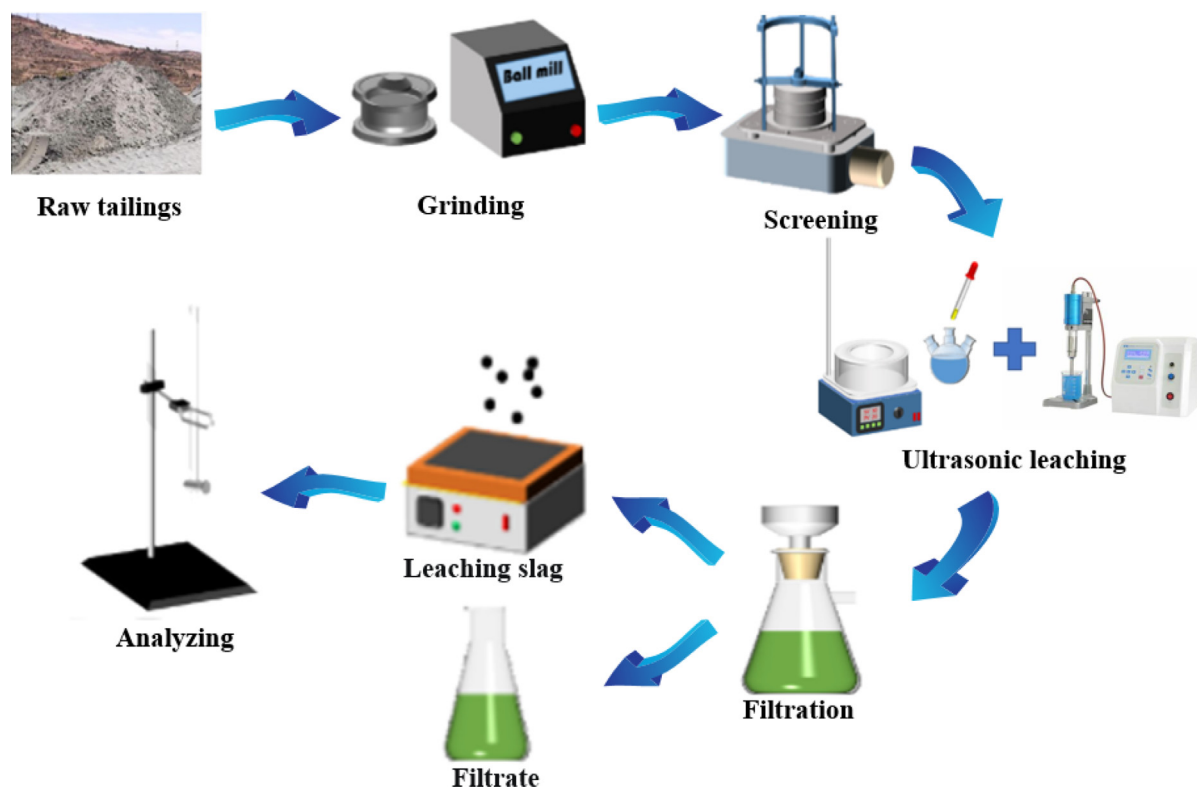


Fig. 4. Process flow chart of the experiment.

was 0.06 s/step, and the step interval was set to 0.02°/step. The scanning structure was analyzed by XRD analysis software x'Pert Highscore with the aid of the PDF-2003 database.

The Thermo ESCALab 250 X-ray photoelectron spectrometer (XPS) was used to analyze the valence state and content of elements in the samples. Injecting X-rays into the sample excited the inner electrons or valence electrons (photoelectrons) of the target element, and the photoelectron energy was measured by the detection system. The photoelectron spectroscopy was obtained through specific calculations, and the relevant information about the samples was obtained.

(3) Morphology analysis

The JSM-6700F cold field emission scanning electron microscope (SEM) (Electronics Company, Japan) and X-Act energy dispersive spectroscopy (EDS) (Oxford Instruments, UK) were used to detect the surface morphology and micro-element distribution of samples. Subsequently, the samples obtained under different conditions were plated with gold or carbon to improve their conductivity, and then these samples were observed in the electron microscope test chamber.

3. Results and discussion

3.1. Thermodynamic analysis

The complexation reaction between vanadium and oxalic acid can be divided into three stages, as depicted in Table 3. The first stage involved the dissolution reaction of V. The main valence states of V in tailings were (IV) and (V). Under the action of H⁺, VO²⁺ and VO₂⁺ were generated, respectively. The specific reactions are shown in Eqs. (1) and (2). The results were consistent with the conclusion obtained by Liu et al. (2020), indicating that vanadium with the valence state of V⁴⁺ and V⁵⁺ mainly existed in the form of VO²⁺ and VO₂⁺ in the inorganic acid solution with a pH value below 1.

The second stage involved the complexation reaction of metal cations. Before the elucidation of the complexation reaction, the anions of oxalic acid were classified. With the continuation of the decomposition reaction, the anions of oxalic acid mainly included HC₂O₄⁻ and C₂O₄²⁻. Based on the known ionization constant K_a (Table 1) of the weak acid, it can be found that the acidity of C₂O₄²⁻ was almost negligible compared with that of HC₂O₄⁻. Hence, it is widely accepted that HC₂O₄⁻ is the main anion in the complexation reaction of oxalic acid (Rezaei et al., 2022). With this understanding, further analysis of the complexation reaction was carried out. In the oxalic acid solution, vanadium oxide ions were combined with oxalic acid and reduced, resulting in the formation of complex anions. Firstly, VO²⁺ formed a complex (VOC₂O₄) under

the complexation of HC₂O₄⁻, and then continued to react under the action of residual oxalate ions to form a new complex (VO(C₂O₄)₂³⁻). The specific reaction can be expressed in Eqs. (1) and (2) (Tracey, 2003). The complexation reaction of VO₂⁺ in the oxalic acid system was similar to that of VO²⁺. The specific complexation products included VO₂C₂O₄⁻ and VO₂(C₂O₄)₂³⁻. The specific reaction can be expressed by Eqs. (5) and (6) (Tracey, 2003).

The third stage involved the reduction reaction of V⁵⁺ complexation anions. VO₂C₂O₄⁻ and VO₂(C₂O₄)₂³⁻ formed VOC₂O₄ and VO(C₂O₄)₂³⁻, respectively, under a series of reductions of HC₂O₄⁻ in the acidic environment (Bruyère et al., 2001). After a series of reactions, the integrated reaction Eqs. (7) and (8) were obtained, which can be simplified to the final reaction Eqs. (9) and (10). Therefore, it can be concluded that VOC₂O₄ and VO(C₂O₄)₂³⁻ were generated by vanadium in the valence states of V⁴⁺ and V⁵⁺, respectively, in the presence of oxalic acid.

The effect of ultrasound in the vanadium complexation reaction process can be intuitively judged through the analysis of the control link in this process. In this regard, a thermodynamic analysis of possible reactions was conducted with the aid of Factsage 8.1, as shown in Fig. 5. Within the temperature range of 293–353 K, the Gibbs free energy was negative in both the first stage and the third stage. Besides, the reaction in the first stage was more prone to occur. This indicates that the first stage and the third stage may proceed spontaneously, and do not play a significant role in the control of the complexation reaction. Within the temperature range of 293–353 K, the Gibbs free energy was positive in the whole reaction in the second stage. This indicates that the reaction tendency in this stage is relatively insignificant, making it a pivotal area of interest in the study of the ultrasonic leaching process for the complexation reaction. On the whole, these reactions can be ranked as follows: the acidolysis of vanadium oxide, the reduction of V⁵⁺ complex anion, and the complexation of vanadium oxide ion with oxalic acid.

3.2. Factors affecting leaching of vanadium from the CRAL tailings

3.2.1. Leaching temperature

During the leaching process, it is crucial to consider the effect of temperature on the efficiency of vanadium leaching. Wu et al. (2018) found that temperatures above 363 K led to the volatilization and decomposition of the oxalic acid solution, resulting in the wastage of leaching agents. To mitigate this issue, a temperature range of 293–353 K was determined for the optimal leaching conditions. In this section, the effect of the leaching temperature on vanadium leaching efficiency was investigated under the oxalic acid concentration of 10%, the liquid–solid ratio of 10:1, the ultrasonic intensity of 20 W/cm², and the stirring speed of 200 rpm for 30 min. The results, as shown in Fig. 6(a), indicated that the vanadium leaching efficiency increased continuously with the rise in

Table 3
List of vanadium leaching reactions.

Step	Chemical reaction equation	Serial number
First stage	$V_2O_5(S) + 2H_3O^+ \leftrightarrow 2VO_2^+ + 3H_2O$	(1)
	$VO_2(S) + 2H_3O^+ \leftrightarrow VO^{2+} + 3H_2O$	(2)
Second stage	$VO^{2+} + HC_2O_4^- + H_2O \leftrightarrow VOC_2O_4 + H_3O^+$	(3)
	$VOC_2O_4 + HC_2O_4^- + H_2O \leftrightarrow VO(C_2O_4)_2^{3-} + H_3O^+$	(4)
	$VO_2^+ + HC_2O_4^- + H_2O \leftrightarrow VO_2(C_2O_4)^{3-} + H_3O^+$	(5)
	$VO_2C_2O_4^- + HC_2O_4^- + H_2O \leftrightarrow VO_2(C_2O_4)_2^{3-} + H_3O^+$	(6)
	$VO_2C_2O_4^- + 2H^+ + HC_2O_4^- = VO(C_2O_4) + H_2O + HC_2O_4^*$	(7)
Third stage	$VO_2(C_2O_4)_2^{3-} + 2H^+ + HC_2O_4^- = VO(C_2O_4)_2^{3-} + H_2O + HC_2O_4^*$	(8)
	$2VO_2C_2O_4^- + 3H^+ + HC_2O_4^- = 2VO(C_2O_4) + 2H_2O + 2CO_2$	(9)
	$2VO_2(C_2O_4)_2^{3-} + 3H^+ + HC_2O_4^- = 2VO(C_2O_4)_2^{3-} + 2H_2O + 2CO_2$	(10)

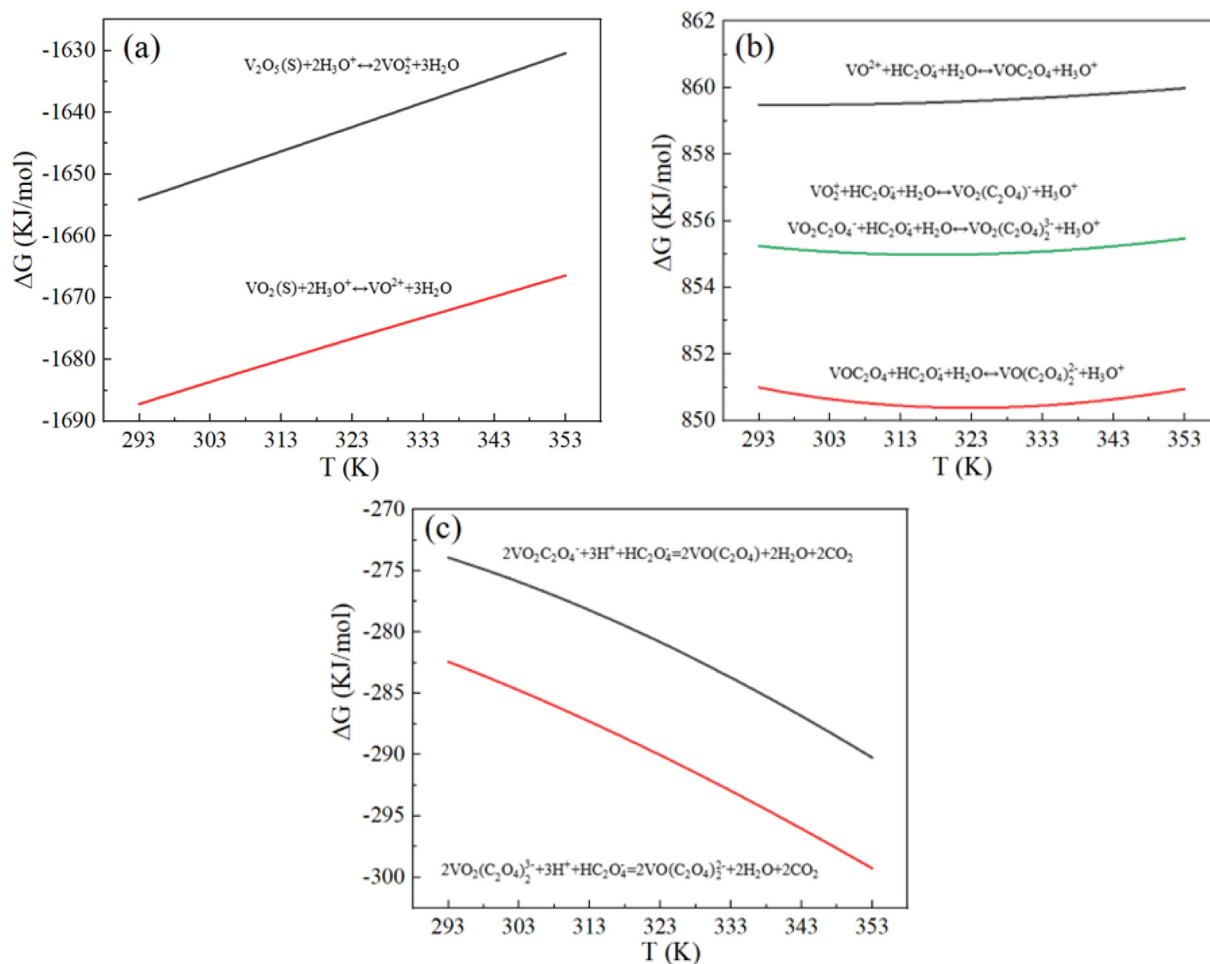
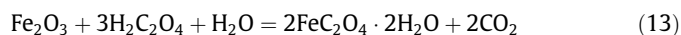
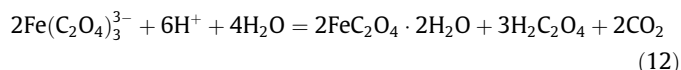


Fig. 5. Thermodynamic analysis of the complexation reaction of vanadium. (a) The first stage; (b) The second stage; (c) The third stage.

leaching temperature. This observation can be attributed to the direct influence of temperature on the reaction rate in chemical reactions. With higher temperatures, the movement rate between molecules increases, leading to more energy and increased collisions per unit interval. Additionally, the proportion of activated molecules increases, which rapidly improves the vanadium leaching efficiency within a short period (Wang et al., 2023). Furthermore, the increase in leaching temperature reduces the viscosity of the solution, enhancing the diffusion coefficient and indirectly accelerating the reaction rate. Comparatively, the ultrasonic leaching efficiency gradually increased within the temperature range of 293–333 K, indicating the beneficial effect of utilizing an appropriate temperature in assisting the ultrasonic leaching process. Under the influence of ultrasound, the solid particle surface's encapsulating boundary layer is effectively broken and stripped, continuously enlarging the reaction area. The temperature rise further elevates the mass transfer rate, enhancing the leaching process. However, when the leaching temperature exceeded 333 K, the increase in ultrasonic rate diminished significantly. This decrease may be attributed to the higher vapor pressure in cavitation bubbles with rising temperature, resulting in an increased threshold for bubble collapse and inhibiting cavitation during the leaching process (Yan et al., 2021). The presence of iron-bearing components, such as hematite, could undergo reactions (11) and (12) in the oxalic acid system, which can merge into reaction (13) (Taxiarhou et al., 1997). According to the research of Kim et al. (2019), the complexation reaction of iron proceeded very slowly when the

leaching temperature was lower than 338 K. With the progression of the reaction, the insoluble ferric oxalate products gradually covered the whole reactant surface layer to prevent the generation of ferric oxalate ions. Based on these findings, the proper temperature for the selective leaching of vanadium was determined to be 333 K.



To fully elucidate the changes of reaction systems in different processes, blank experiments on the oxalic acid solution were conducted. The results, as depicted in Fig. 6(b), revealed a continuous increase in the decomposition amount of oxalic acid with rising leaching temperatures. Furthermore, ultrasound treatment facilitated higher decomposition efficiency. In an aqueous solution, oxalic acid underwent gradual decomposition, as indicated by the following reactions (14) and (15). The ionization constant of acetic acid in the decomposition process was only 1.75×10^{-5} , which had negligible influence on the oxalic acid complexation process. The decomposition of oxalic acid resulted in significant costs, thus emphasizing the need to maximize the utilization of decomposition products in industrial production. Under the influence of ultrasound, some oxalic acid molecules may react with hydroxyl

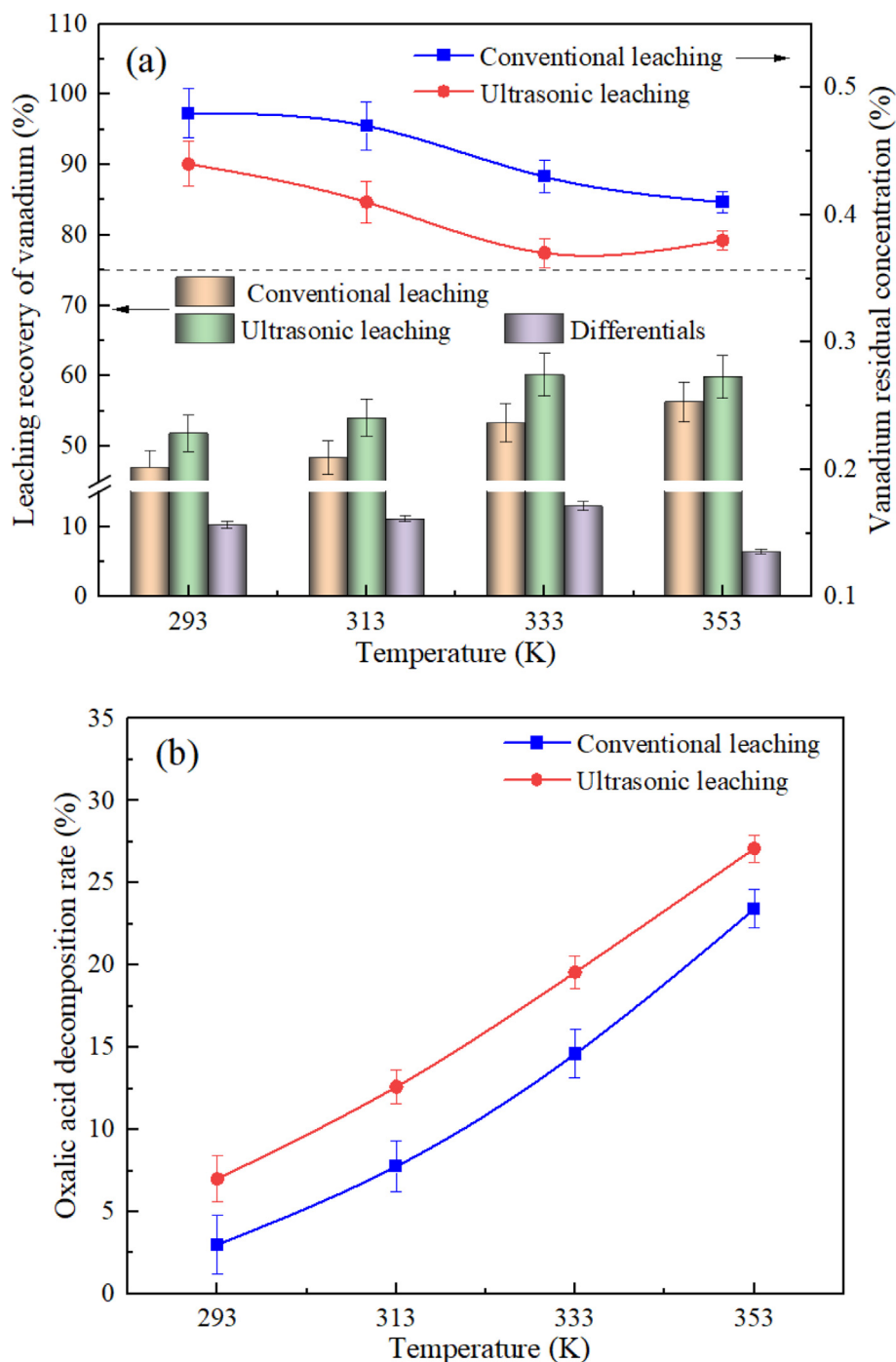
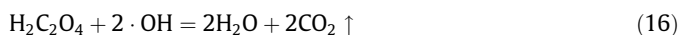
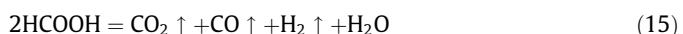
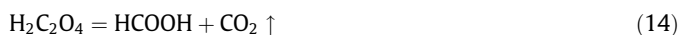


Fig. 6. Effect of the leaching temperature on the vanadium leaching efficiency (a) and the oxalic acid decomposition rate (b) under different processes.

radicals ($\cdot\text{OH}$) to generate numerous bubbles, as shown in Eq. (16) (Kim et al., 2019). When the adding amount of oxalic acid was fixed, the number of bubbles produced under the action of ultrasound was larger than that produced by the conventional leaching process. Additionally, most of these bubbles served as nucleation sites to enhance cavitation.



3.2.2. Oxalic acid concentration

In this section, the effect of the oxalic acid concentration on vanadium leaching efficiency was investigated under the leaching temperature of 333 K, the liquid–solid ratio of 10:1, the ultrasonic intensity of 20 W/cm², and the stirring speed of 200 rpm for 30 min. The results are shown in Fig. 7(a). The results indicated that as the oxalic acid concentration increased, the vanadium leaching efficiency displayed an upward trend, especially within the range of 1%–5%. This can be attributed to the enhanced reaction between the high-concentration leaching solution and the solid particle surface binding site. Notably, the leaching efficiency of

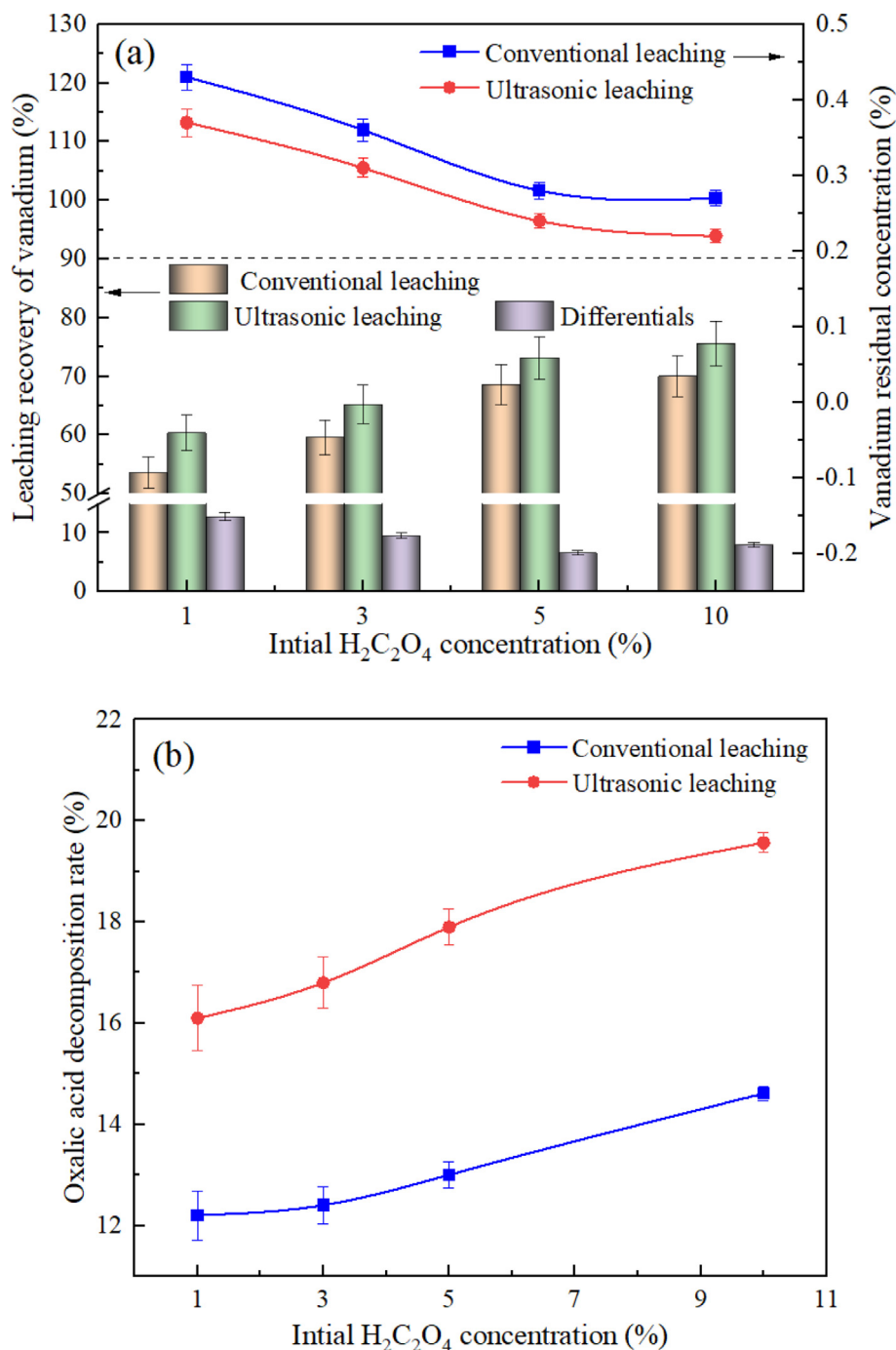


Fig. 7. Effect of the oxalic acid concentration on the vanadium leaching efficiency (a) and the oxalic acid decomposition rate (b) under different processes.

the two processes increased by 15.10% and 12.07%, respectively, when the oxalic acid concentration increased from 3% to 5%. This indicates the highest increase in leaching efficiency with changes in oxalic acid concentration. However, when the oxalic acid concentration exceeded 5%, the increase rate of the leaching efficiency began to slow down. This indicated that the high-concentration oxalic acid system does not contribute to further improvement in leaching efficiency. This can be explained by the limited binding sites exposed in the solution that can react with oxalic acid, causing the control mechanism to shift from chemical reactions to diffusion. At an oxalic acid concentration of 5%, the leaching efficiency of vanadium reached 68.59% and 73.14%, respectively, under conventional and ultrasonic leaching scenarios. On that basis, the opti-

mal oxalic acid concentration was determined to be 5%, regardless of conventional leaching or ultrasonic leaching. Compared with the conventional process, the ultrasonic enhanced process can enhance the vanadium leaching process from the raw tailings under different oxalic acid concentrations. The difference in leaching efficiency between the two processes gradually decreased as the leaching system concentration increased from 1% to 5%. This can be attributed to the continuous increase in viscosity with increasing oxalic acid concentration, which resulted in the weakening of cavitation effects (Xu et al., 2023).

Furthermore, the relationship between the oxalic acid concentration and the oxalic acid decomposition rate was examined, as shown in Fig. 7(b). The results revealed that changes in oxalic acid

concentration had minimal impact on the decomposition rate in the conventional leaching process. However, in the ultrasonic leaching process, an increase in oxalic acid concentration led to an improvement in oxalic acid decomposition rate, although the rate of improvement gradually decelerated. Within the range of 5% to 10% oxalic acid concentration, further increasing the concentration resulted in a rise in the difference value. This can be explained by the increased bubble generation due to oxalic acid decomposition under the influence of ultrasound, which ensured cavitation. In contrast, under conventional conditions, the reaction diffusion decelerated due to changes in system viscosity, compromising the leaching efficiency.

3.2.3. Ultrasonic intensity

Ultrasonic intensity (W/cm^2) refers to the acoustic energy per unit area in a unit interval. It can be regarded as the energy acting on the leaching system. Hence, the ultrasonic intensity would exert significant impacts on the ultrasonic efficiency. In this section, the effect of the ultrasonic intensity on vanadium leaching efficiency was investigated under the leaching temperature of 333 K, the oxalic acid concentration of 5%, the liquid–solid ratio of 10:1, and the stirring speed of 200 rpm for 30 min. The results are shown in Fig. 8 (a). With the continuous increase of the ultrasonic intensity, the increase rate of the vanadium leaching efficiency gradually decelerated. When the ultrasonic intensity increased from 20 W/cm^2

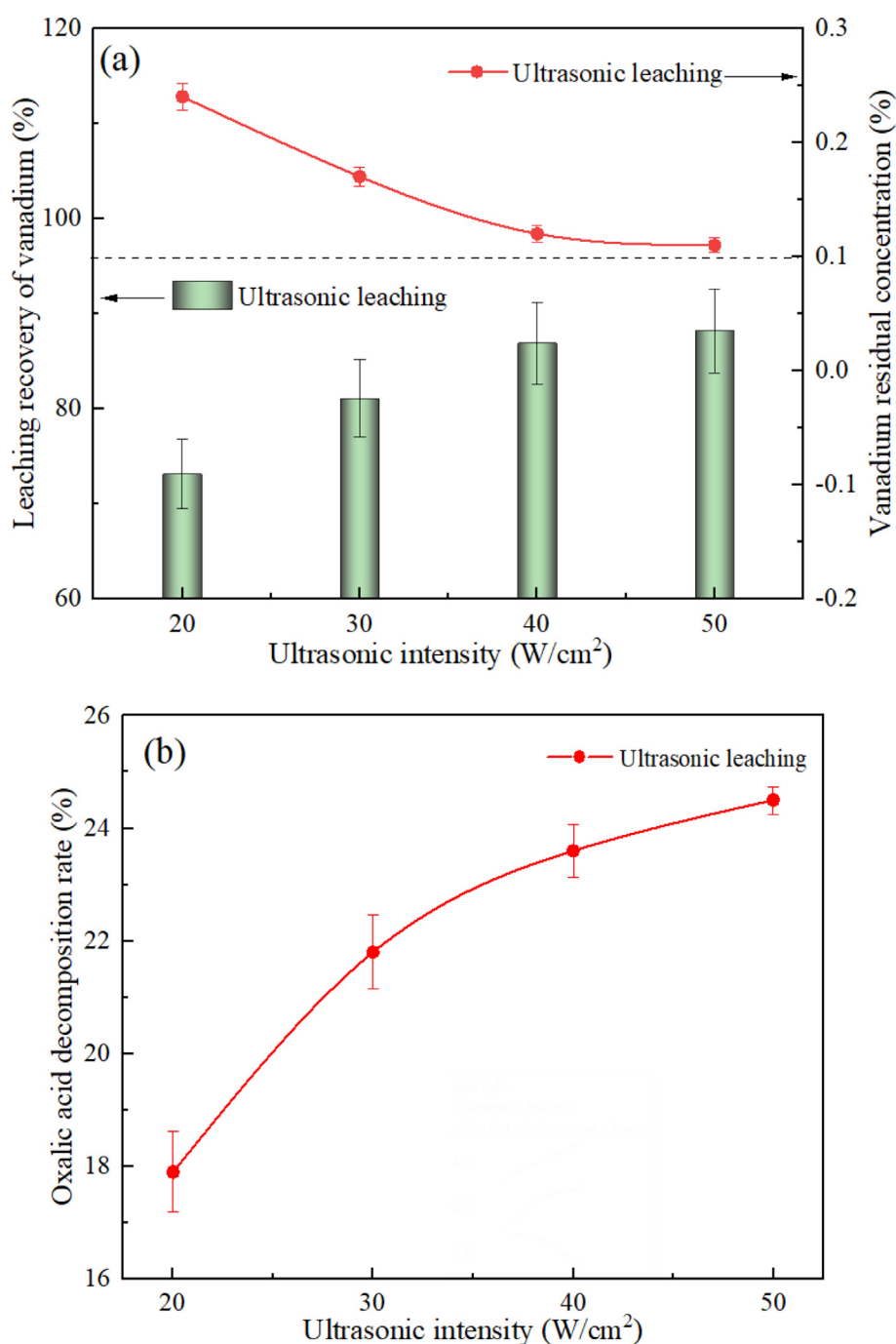


Fig. 8. Effect of the ultrasonic intensity on the vanadium leaching efficiency (a) and the oxalic acid decomposition rate (b) under different processes.

to 40 W/cm², the vanadium leaching efficiency increased from 73.14% to 86.88%. This can be attributed to the generation of more cavitation bubble nuclei in the solution, leading to enhanced cavitation effects induced by ultrasound (Xu et al., 2023). The enhancement of cavitation contributed to the stirring of the solution, which accelerated the heterogeneous reaction rate and the diffusion of reactants and products. When the ultrasonic intensity exceeded 40 W/cm², the leaching efficiency remained basically unchanged. After the cavitation intensity reached a certain degree, cavitation tended to the saturation state. Under this circumstance, increasing the ultrasonic intensity would generate numerous ineffective bubbles, thus forming a sound shielding phenomenon and reducing the available sound field energy of the system (Liu et al., 2022). Based on the vanadium leaching efficiency, the optimal ultrasonic intensity was determined to be 40 W/cm².

Meanwhile, the effect of the ultrasonic intensity on the oxalic acid decomposition rate was also examined, as shown in Fig. 8 (b). With the increase of the ultrasonic intensity, the increase pat-

tern of the oxalic acid decomposition rate was similar to that of the vanadium leaching efficiency. The thermal effect caused by cavitation in the ultrasonic process generated a local high temperature, which directly induced the decomposition of oxalic acid in the oxalic acid solution with high-temperature instability (Lin et al., 2022). Subsequently, with the attenuation of cavitation, the area of the high-temperature area tended to be saturated, and the increase trend of the oxalic acid decomposition rate also decelerated.

Moreover, the SEM analysis was performed to explore the microstructure of raw tailings and leaching residues from different processes (Fig. 9). There were significant differences in the microstructure of raw tailings and leaching residues under the action of ultrasound. The raw tailings had a compact structure, accompanied by the severe and irregular symbiosis phenomenon, which was similar to the conventional leaching residues. Under the action of ultrasound, the average particle size of leaching residues decreased significantly. Besides, the nesting phenomenon of different minerals was also improved, which indicated that ultra-

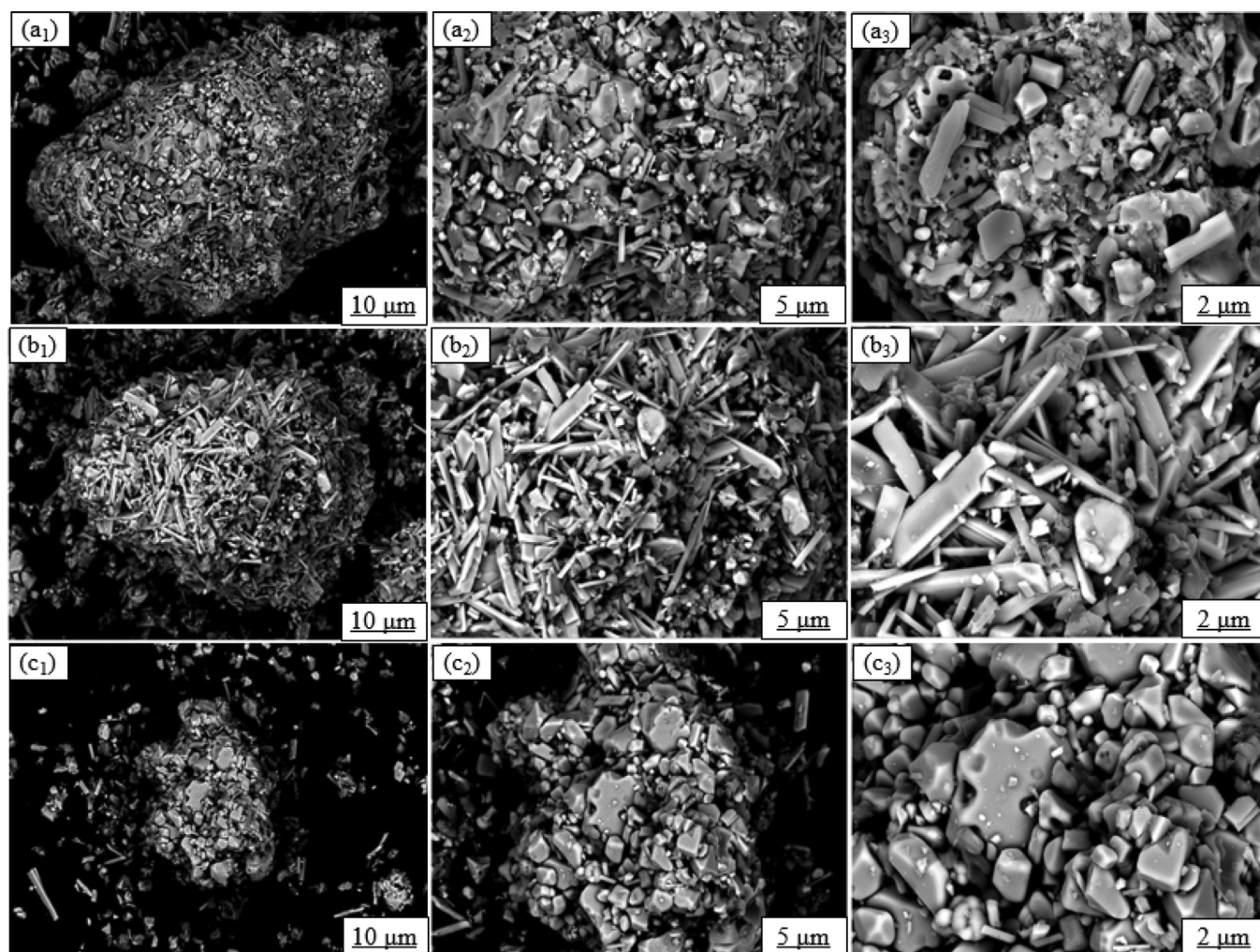


Fig. 9. SEM images of raw tailings and leaching residues. (wt%) ((a) Raw tailings; (b) Conventional leaching residues; (c) Ultrasonic leaching residues).

Table 4

Comparison of elements contents of raw tailings and leaching residues. (wt%) ((a) raw tailings; (b) conventional leaching residues; (c) Ultrasonic leaching residues).

Elements		Fe	Mn	Cr	Ca	Ti	Si	S	V
Contents	(a)	37.93	15.00	11.54	9.36	9.27	7.33	6	0.84
	(b)	40.93	15.91	12.34	9.96	9.81	7.65	0.05	0.28
	(c)	41.21	15.97	12.42	9.99	9.84	7.24	0.04	0.12

sound exerted a significant impact on the stripping and dispersion of minerals (Liu et al., 2021c).

3.3. Characterization of leaching residues

The composition of raw tailings and leaching residues was analyzed using XRF and XRD techniques, and the results are presented in Table 4 and Fig. 10. The main components identified in the raw tailings were Fe_2O_3 , $\text{CaSO}_4 \cdot (\text{H}_2\text{O})_2$, MnCr_2O_4 , FeTiO_3 , and SiO_2 . Similarly, the leaching residues consisted primarily of Fe_2O_3 , $\text{CaC}_2\text{O}_4 \cdot \text{H}_2\text{O}$, MnCr_2O_4 , FeTiO_3 , and SiO_2 . Interestingly, the phase diffraction peak intensity of leaching residues was not significantly attenuated compared with that of raw tailings. This suggests that the use of cavitation may not be effective in further disrupting the internal mineral structure when there is an abundance of fine particles ($\geq 200 \mu\text{m}$) present in the industrial tailings being used as raw materials. As shown in chemical Eq. (17), $\text{CaSO}_4 \cdot (\text{H}_2\text{O})_2$ was converted into $\text{CaC}_2\text{O}_4 \cdot \text{H}_2\text{O}$. The sulfur in the slag exists in two forms: the free state (SO^{2-}) and the combined state (CaSO_4). SO^{2-} is the residual acid component after industrial acid leaching, while CaSO_4 originally existed within the slag. During the experimental progress, SO^{2-} effectively entered the leaching solution, while CaSO_4 reacted with $\text{H}_2\text{C}_2\text{O}_4$ to produce CaC_2O_4 precipitation. Furthermore, the presence of Fe in the leaching residues from both processes showed varying degrees of enrichment, facilitating the subsequent reuse of leaching residues in ironmaking.



In addition, the surface scan analysis (Fig. 11) also detected the presence of Fe, Mn, Cr, Ca, Ti, Si, S, and V in the leaching residues, which was consistent with the result measured by XRF. Notably, the agglomeration area of elements other than Fe was significantly diminished in the ultrasonic leaching residues compared to the conventional ones. This can be attributed to the shear stress caused by the collapse of cavitation bubbles under the action of ultrasound, which destroyed and stripped off the surface layers of different phases, thus exposing inclusions such as gangue (Verma et al., 2021). Under this circumstance, oxalic acid was prone to contact with V in the Ca phase and the Si phase through cracks and

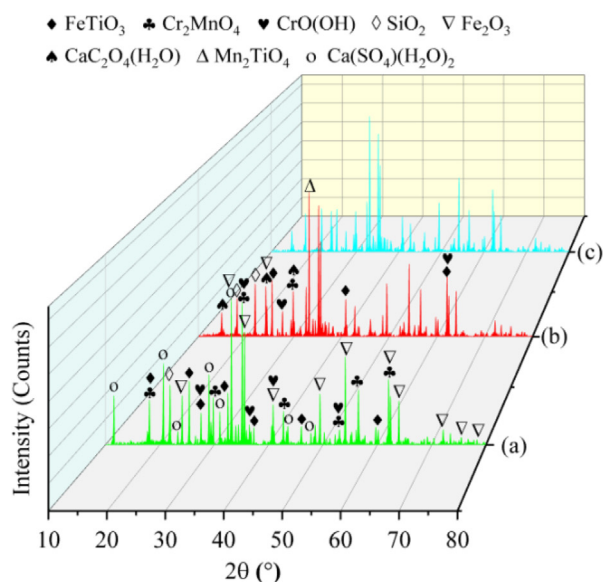
pores. Therefore, the application of ultrasound enlarged the reaction interface, improved the contact between solid and liquid, and accelerated the reaction rate.

The occurrence state of the main elements in raw tailings under the action of oxalic acid and ultrasound was analyzed by XPS (Fig. 12). The similar elements between leaching residues and raw tailings mainly included Fe2p, O1s, and Ti2p. The distribution of the characteristic peaks of Fe and V in the leaching residues was similar to that of raw tailings. The characteristic peaks of both were located at 734.0 eV, 729.8 eV, 726.2 eV, and 723.8 eV (Fe2p1/2) and 719.9 eV, 716.7 eV, 712.8 eV, and 710.4 eV (Fe2p3/2); 524.3 eV and 523.0 eV (V2p1/2) and 517.1 eV and 516.0 eV (V2p3/2), respectively (Wu et al., 2023; Jenifer and Sriram, 2023).

The intensity of iron diffraction peaks in leaching residue exhibited slight changes compared with that in raw tailings. Additionally, both conventional and ultrasonic leaching residues displayed a similar content of iron in different valence states, suggesting that the Fe-bearing phase had minimal participation in the pure oxalic acid system reaction. In contrast, the significantly increased content of Fe^{3+} in ultrasonic leaching residues suggested that the oxidation potential of the leaching system was improved under the action of ultrasound. As a result, compact ilmenite was converted into loose iron oxide, facilitating the stripping and dispersion of mineral particles. Notably, the intensity of vanadium diffraction peaks in the leaching residues exhibited a significant reduction in comparison to the raw tailings, specifically in terms of V^{5+} . This observation indicated that V^{5+} in raw tailings had a low encapsulation degree compared with V^{4+} , which was beneficial to the leaching and recovery of V^{5+} . Moreover, the analysis of vanadium content in different valence states revealed a similar proportion of vanadium in the tailings. Both V^{4+} and V^{5+} accounted for roughly half of the total content, while a portion of vanadium with various valence states remained encapsulated.

3.4. Mechanism analysis

Based on a comparative analysis of different leaching processes, this study aimed to summarize the mechanism of ultrasound in the CRAL tailings. The initial analysis of the conventional leaching process revealed that vanadium mainly existed in calcium sulfate col-



Phase	(a)	(b)	(c)
Fe_2O_3	29.6	34.2	39.8
$\text{CaSO}_4 \cdot (\text{H}_2\text{O})_2$	24.6		
MnCr_2O_4	19.0	17.6	17.3
FeTiO_3	16.6	15.1	14.6
SiO_2	8.1	8.0	7.0
$\text{Mn}_2(\text{TiO}_4)$		2.3	2.5
$\text{CrO}(\text{OH})$	2.1	1.9	3.0
$\text{CaC}_2\text{O}_4 \cdot \text{H}_2\text{O}$		19.1	18.8

Fig. 10. Phase comparison of raw tailings and leaching residues (wt%). ((a) Raw tailings; (b) Conventional leaching residues; (c) Ultrasonic leaching residues).

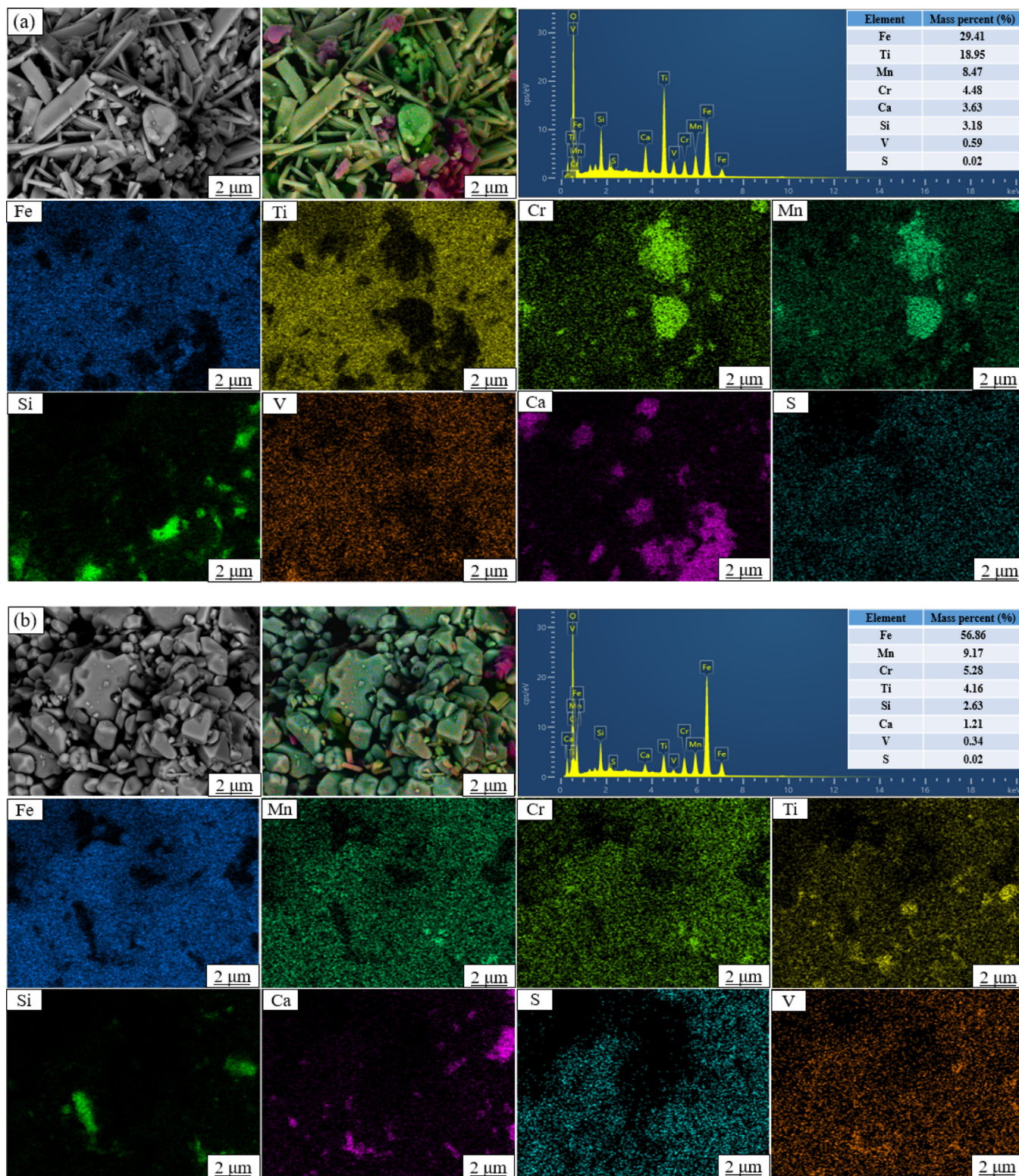


Fig. 11. Backscattering diagram and element distribution diagram of different leaching residues. ((a) Conventional leaching residues; (b) Ultrasonic leaching residues).

loid and gangue in raw tailings. After complexation with oxalate ions, the colloid transformed into calcium oxalate precipitation. The residual vanadium adsorbed by the colloid was converted into water-soluble vanadium ions in the acidic environment, which then reacted with oxalate ions. However, the gangue did not react with acidic substances, leading to the retention of some vanadium within its lattice structure, thereby hindering its release during the

complexation reaction. Additionally, the slow diffusion in the conventional leaching process resulted in the unnecessary decomposition of some oxalic acid at high temperatures, thereby increasing production costs.

The introduction of ultrasound in the leaching process triggers a chemical reaction due to the collapse of microbubbles under cavitation. This reaction generates highly active free radicals known as

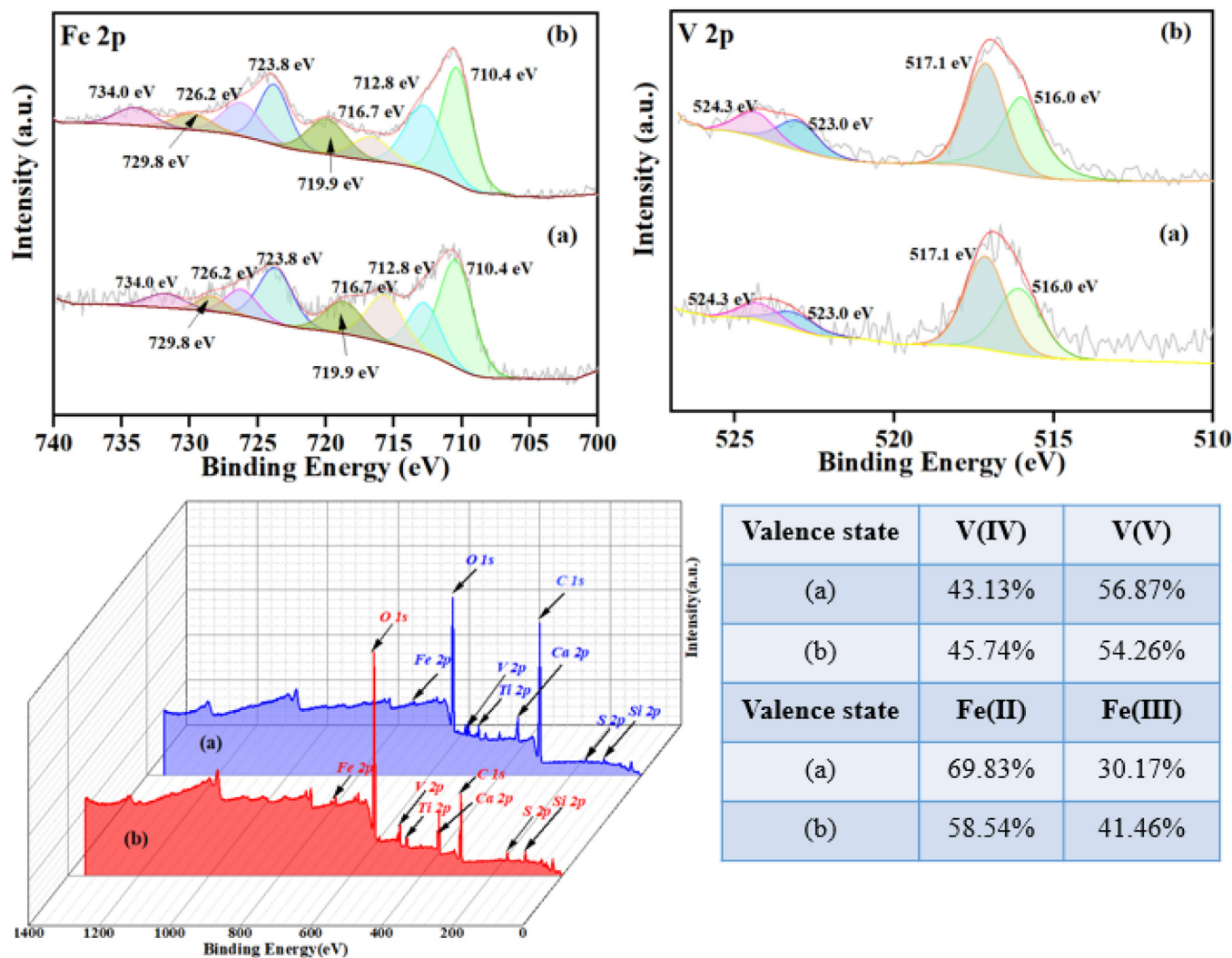


Fig. 12. XPS spectra of leaching residues and the distribution of Fe and V contents in each valence state. ((a) Conventional leaching residues; (b) Ultrasonic leaching residues).

Table 5
Expression of mechanism analysis.

Chemical equation	Serial number
$H_2O + \gamma \rightarrow H \cdot + HO \cdot$	(18)
$H \cdot + H \cdot \rightarrow H_2$	(19)
$H^+ + H_2O + \gamma \rightarrow HO \cdot + H_2$	(20)

hydroxyl radicals ($\cdot OH$) that possess strong oxidation ability but weak selectivity. The oxidation ability of $\cdot OH$ is second only to fluorine, as its standard electrode potential is 2.8 eV. Consequently, the introduction of $\cdot OH$ effectively alleviates the control limitation in the complexation reaction. By selectively targeting the elements in the tailings, the addition of $\cdot OH$ can facilitate the oxidative leaching reaction when combined with oxalic acid. The generation of $\cdot OH$ in the complexation reaction involves two main sources. Firstly, under the influence of ultrasound, $\cdot OH$ is produced through the decomposition of water molecules, as depicted in chemical Eqs. (18) and (19) in Table 5. Secondly, $\cdot OH$ is generated from the reaction between hydrogen ions and water molecules under the influence of ultrasound, as expressed in Eq. (20) (Chen et al., 2020).

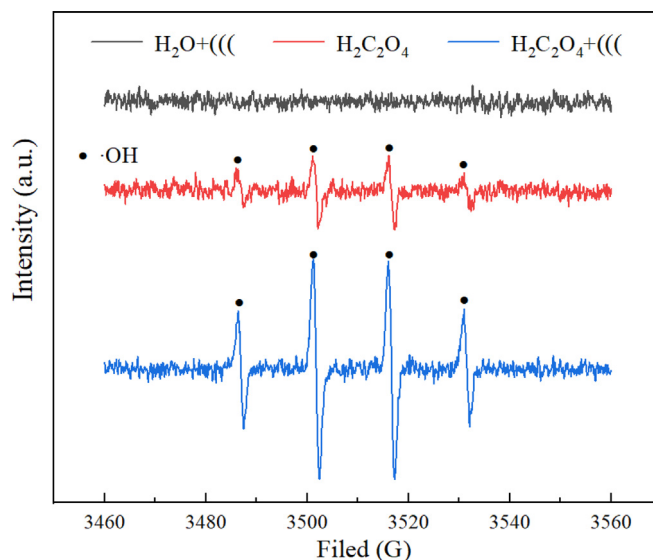


Fig. 13. EPR spectra in different leaching systems.

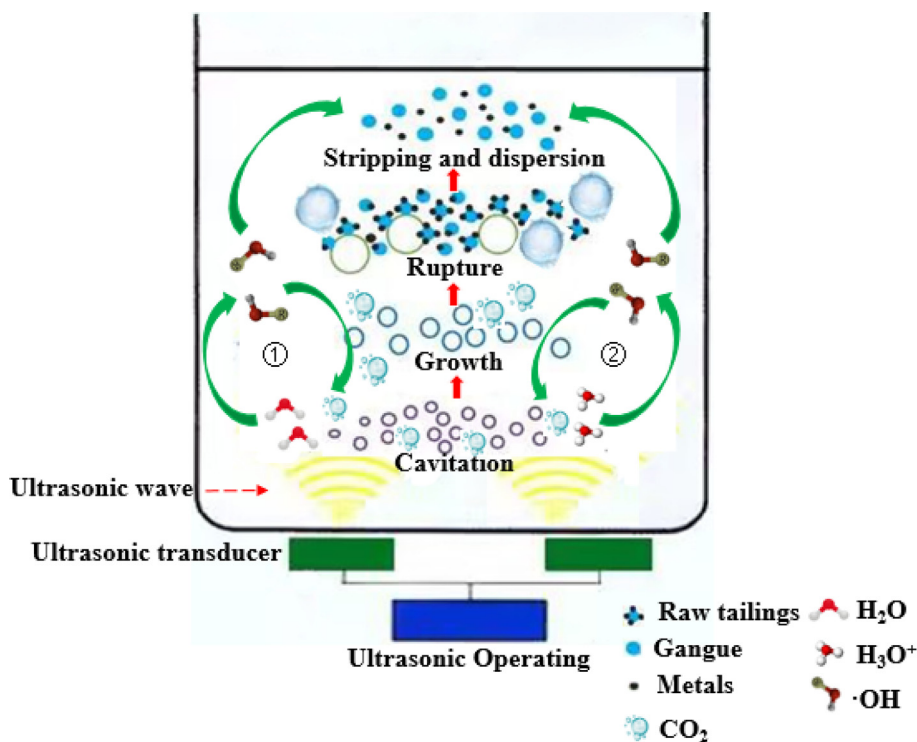


Fig. 14. The mechanism of ultrasound in the complexation reaction of raw tailings.

To investigate the chemical impact of ultrasonic waves on the leaching process, Electron Paramagnetic Resonance (EPR) was employed to decipher the formation pattern of OH in various leaching systems under optimal ultrasonic leaching conditions. As depicted in Fig. 13, the application of ultrasound in the distilled water system yielded an inconspicuous ·OH signal, possibly due to the low ultrasonic power. However, upon the addition of H₂C₂O₄, a distinct ·OH characteristic peak materialized in the original system under ultrasonic influence. To determine the primary source of OH, the generation of OH radicals in the H₂C₂O₄ solution sans ultrasonic intervention was examined. Although the inclusion of H₂C₂O₄ resulted in a stronger ·OH signal, it did not match the intensity observed with ultrasonic treatment. This indicates that H₂C₂O₄ can autonomously produce ·OH under heated conditions, albeit in limited quantities. Ultrasonic waves, on the other hand, effectively enhance the oxidation reaction of H₂C₂O₄ by inducing cavitation effects, facilitating the entry of the reaction system into a supercritical state, and promoting the efficient decomposition of H₂C₂O₄, leading to the generation of OH radicals.

Given the limitations of the conventional leaching process, this study aims to explore the potential benefits of ultrasound in the leaching process. As shown in Fig. 14, the mechanism of ultrasound was investigated in detail. Two primary pathways were identified for the generation of hydroxyl radicals (·OH) in the oxalic acid system under ultrasound irradiation. Firstly, ultrasound can directly decompose H₂O in the solution to generate OH. This process significantly enhances the oxidation environment of the reaction. Secondly, under the action of ultrasound, the acidic environment facilitates the decomposition of hydronium ions H₃O⁺ into ·OH. This further contributes to the generation of ·OH and the improvement of the reaction conditions. The generation of ·OH is not only advantageous for the oxidation environment but also plays a crucial role in the direct reaction with oxalic acid. This leads to the release of numerous carbon dioxide (CO₂) bubbles. These bubbles, originating from both the CO₂ in the solution and the CO₂ attached to the mineral surface, act as nuclei for bubble formation. The con-

tinuous growth of these bubbles, influenced by the phenomenon of cavitation, ultimately leads to their collapse and rupture. Consequently, micro-jets are formed, which effectively destroy the mineral surface and accelerate the mass transfer process. Additionally, the local high temperature and high pressure induced by ultrasound contribute to the enhanced nesting phenomenon of symbiotic tailings. Consequently, the chemical reaction process is accelerated. Furthermore, ultrasound exhibits both a perturbation effect and an energy gathering effect. These effects collectively lead to a reduction in the activation energy of the reaction, promoting the generation of ·OH and facilitating the continuous oxalic acid decomposition cycle. Ultimately, this improves the conditions of complexation reactions.

4. Conclusion

In this study, a novel method, known as ultrasonic enhanced oxalic acid complexation, was utilized to effectively remove residual vanadium from calcification roasting-acid leaching tailings. The main conclusions are as follows:

- (1) Ultrasonic enhanced oxalic acid complexation significantly improves vanadium removal efficiency. Under the optimal conditions of temperature 333 K, oxalic acid concentration 5%, liquid–solid ratio 10:1, ultrasonic intensity 40 W/cm², stirring speed 200 rpm and stirring time 30 min, the removal rate of vanadium and the decomposition rate of oxalic acid reached 86.88% and 23.6%, respectively, which were significantly higher than the corresponding values achieved by the conventional method (The removal rate of vanadium increased by 26.67%, and the decomposition rate of oxalic acid by 81.54%). By extracting a majority of the vanadium from the slag, this method reduces environmental pollution and provides valuable vanadium metal for industrial applications. This study serves as a theoretical foundation for the advancement of vanadium industrial production.

- (2) The acidity of leaching environment is a key factor affecting the leaching efficiency. In the conventional leaching process, oxalic acid decomposes into acetic acid, which compromises the effect of complexation between oxalic acid and vanadium. Ultrasonic cavitation generates $\cdot\text{OH}$, which minimizes the formation of acetic acid. Additionally, and under strong oxidation potential, oxalic acid directly decomposes to produce a large number of CO_2 bubbles. Some of these bubbles firmly adhere to the surface of the original tailings and the solution, supplementing the limited bubble nucleuses generated by cavitation, thus directly enhancing the cavitation effect and providing enough $\cdot\text{OH}$ in a virtuous cycle during the ultrasonic leaching process.
- (3) The virtuous cycle, with the $\cdot\text{OH}$ generated by cavitation continuously participating in the decomposition of oxalic acid to produce more CO_2 bubbles as cavitation bubble nuclei, fuels the ultrasonic leaching process. The strengthened cavitation effect occurs due to the ultrasonic waves acting on the interface between the leaching agent and the material particles, generating micro-jets that accelerate the destruction of inclusions and promote mass transfer. Simultaneously, local high temperatures and pressures facilitate the stripping and dispersion of associated tailings. Furthermore, the micro-disturbance effect and energy accumulation reduce the activation energy required for reactions. These factors optimize complexation conditions and accelerate chemical reactions.

Overall, the ultrasonic enhanced oxalic acid complexation method demonstrates great promise for efficient vanadium removal from calcification roasting-acid leaching tailings. Its ability to enhance vanadium removal efficiency, reduce environmental pollution, and provide valuable vanadium metal holds immense potential for industrial applications.

CRediT authorship contribution statement

Haoyu Li: Writing – original draft, Supervision. **Qian Ren:** . **Shihong Tian:** Investigation, Validation. **Jun Wang:** Writing – review & editing. **Xuejun Zhu:** Data curation, Software. **Tao Yang:** . **Yi Zhang:** Methodology, Conceptualization. **Jingjing Liu:** . **Jiayuan Liu:** .

Declaration of Competing Interest

The authors declare that they have no known competing financial interests or personal relationships that could have appeared to influence the work reported in this paper.

Acknowledgments

This work was supported by Research Project of Panzhuhua University (202201), Ph.D. Research Start-up Funding Project of Panzhuhua University (bkqj2021009) and Innovation and entrepreneurship training program for college students (202311360015).

References

Arif, A.B., Susanto, S., Widayanti, S.M., Matra, D.D., 2023. Pre-storage oxalic acid treatment inhibits postharvest browning symptoms and maintains quality of abiu (*Pouteria caimito*) fruit. *Sci. Hortic-Amsterdam* 311, 111795.

Bruyère, V.I.E., García Rodenas, L.A., Morando, P.J., Blesa, M.A., 2001. Reduction of vanadium(V) by oxalic acid in aqueous acid solutions. *J. Chem. Soc. Dalton Trans.* 24, 3593–3597.

Chen, B., Bao, S., Zhang, Y., 2021. Synergetic strengthening mechanism of ultrasound combined with calcium fluoride towards vanadium extraction from low-grade vanadium-bearing shale. *Int. J. Min. Sci. Techno.* 31 (6), 1095–1106.

Chen, X., Li, S., Wu, X., Zhou, T., Ma, H., 2020. In-situ recycling of coating materials and Al foils from spent lithium ion batteries by ultrasonic-assisted acid scrubbing. *J. Clean. Prod.* 258, 120943.

Cheng, J., Yi, L., Hai, D., Chen, X., Diao, J., Xie, B., 2023. Magnesian roasting kinetics exploration of vanadium slag toward minimization of tailing toxicity. *J. Hazard. Mater.* 452, 131378.

Esmaili, M., Rastegar, S.O., Beigzadeh, R., Gu, T., 2020. Ultrasound-assisted leaching of spent lithium ion batteries by natural organic acids and H_2O_2 . *Chemosphere* 254, 126670.

Guo, X., Chen, S., Han, Y., Hao, C., Feng, X., Zhang, B., 2023. Bioleaching performance of vanadium-bearing smelting ash by *Acidithiobacillus ferrooxidans* for vanadium recovery. *J. Environ. Manage.* 336, 117615.

Hu, P., Zhang, Y., Liu, H., Liu, T., Li, S., Zhang, R., Guo, Z., 2023. High efficient vanadium extraction from vanadium slag using an enhanced acid leaching-coprecipitation process. *Sep. Purif. Technol.* 304, 122319.

Jenifer, A., Sriram, S., 2023. Enhanced photocatalytic organic dye degradation activities of pristine and Zn-doped V_2O_5 nanoparticles. *Appl. Surf. Sci.* 611, 155629.

John, Y., 2006. *Chem. Eng. Res. Des.* 84 (5), 416.

Kim, J.H., Lee, H.K., Park, Y.J., Lee, S.B., Choi, S.J., Oh, W., Kim, H.S., Kim, C.R., Kim, K.C., Seo, B.C., 2019. Studies on decomposition behavior of oxalic acid waste by UVC photo-Fenton advanced oxidation process. *Nucl. Eng. Technol.* 51 (8), 1957–1963.

Lee, J., Kurniawan, E.K., Chung, K.W., Kim, R., Jeon, H., 2021. A review on the metallurgical recycling of vanadium from slags: towards a sustainable vanadium production. *J. Mater. Res. Technol.* 12, 343–364.

Li, K., Jiang, Q., Gao, L., Chen, J., Peng, J., Koppala, S., Omran, M., Chen, G., 2020. Investigations on the microwave absorption properties and thermal behavior of vanadium slag: Improvement in microwave oxidation roasting for recycling vanadium and chromium. *J. Hazard. Mater.* 395, 122698.

Li, M., Liu, C., Ding, A., Xiao, C., 2023. A review on the extraction and recovery of critical metals using molten salt electrolysis. *J. Environ. Chem. Eng.* 11, 109746.

Li, W., Yan, X., Niu, Z., Zhu, X., 2021. Selective recovery of vanadium from red mud by leaching with using oxalic acid and sodium sulfite. *J. Environ. Chem. Eng.* 9 (4), 105669.

Lin, G., Li, J., Zeng, B., Wang, W., Li, C., Zhang, L., 2022. Leaching of rubidium from biotite ore by chlorination roasting and ultrasonic enhancement. *Arab. J. Chem.* 15 (11), 104275.

Liu, S., Ding, E., Ning, P., Xie, G., Yang, N., 2021a. Vanadium extraction from roasted vanadium-bearing steel slag via pressure acid leaching. *J. Environ. Chem. Eng.* 9 (3), 105195.

Liu, Z., Huang, J., Zhang, Y., Liu, T., Hu, P., Liu, H., Zheng, Q., 2020. Separation and recovery of iron impurities from a complex oxalic acid solution containing vanadium by $\text{K}_3\text{Fe}(\text{C}_2\text{O}_4)_3 \cdot 3\text{H}_2\text{O}$ crystallization. *Sep. Purif. Technol.* 232, 115970.

Liu, Q., Tu, T., Guo, H., Cheng, H., Wang, X., 2021b. High-efficiency simultaneous extraction of rare earth elements and iron from NdFeB waste by oxalic acid leaching. *J. Rare Earths.* 39 (3), 323–330.

Liu, J., Wang, S., Liu, C., Zhang, L., Kong, D., 2021c. Mechanism and kinetics of synergistic decopperization from copper anode slime by ultrasound and ozone. *J. Clean. Prod.* 322, 129058.

Liu, H., Zhang, Y., Liu, T., Huang, J., Chen, L., Hu, Y., 2023. Preparation of vanadium electrolyte from vanadium shale leaching solution with high concentration chloride using D2EHPA. *T. Nonferr. Metal. Soc.* 33 (5), 1594–1608.

Ma, M., Wang, W., Li, J., Zhang, K., He, X., 2023. Experimental study of the activation effect of oxalic acid on the dissolution of rare earth elements in the typical diagenetic minerals of coal seams. *Minerals* 13 (4), 525.

Mohanty, C., Behera, S.S., Marandi, B., Tripathy, S.K., Parhi, P.K., Sanjay, K., 2021. Citric acid mediated leaching kinetics study and comprehensive investigation on extraction of vanadium (V) from the spent catalyst. *Sep. Purif. Technol.* 276, 119377.

Opferkuch, K., Caeiro, S., Salomone, R., Ramos, T.B., 2021. Circular economy in corporate sustainability reporting: A review of organisational approaches. *Bus. Strateg. Environ.* 30 (8), 4015–4036.

Peng, H., 2019. A literature review on leaching and recovery of vanadium. *J. Environ. Chem. Eng.* 7 (5), 103313.

Petranikova, M., Tkaczyk, A.H., Bartl, A., Amato, A., Lapkovskis, V., Tunsu, C., 2020. Vanadium sustainability in the context of innovative recycling and sourcing development. *Waste Manag.* 113, 521–544.

Rezaei, H., Shafaei, S.Z., Abdollahi, H., Shahidi, A., Ghassa, S., 2022. A sustainable method for germanium, vanadium and lithium extraction from coal fly ash: Sodium salts roasting and organic acids leaching. *Fuel* 312, 122844.

Rouquette, L.M., Petranikova, M., Vieceli, N., 2023. Complete and selective recovery of lithium from EV lithium-ion batteries: modeling and optimization using oxalic acid as a leaching agent. *Sep. Purif. Technol.*, 124143.

Taxiarchou, M., Panias, D., Douni, I., Paspaliaris, I., Kontopoulos, A., 1997. Removal of iron from silica sand by leaching with oxalic acid. *Hydrometall.* 46, 215–227.

Tracey, A.S., 2003. Applications of 51V NMR spectroscopy to studies of the complexation of vanadium (V) by α -hydroxycarboxylic acids. *Coord. Chem. Rev.* 237, 113–121.

Verma, P., Singh, P., Roy, P.K., 2021. Influence on properties of $\text{Bi}_{0.9}\text{Sm}_{0.1}\text{FeO}_3$ multiferroic system with Mg substitution at Fe-site. *J. Solid State Chem.* 302, 122432.

- Wang, Z., Peng, Z., Li, Y., Zhu, Y., Xie, K., 2023. Selective sulfuric acid cyclic leaching of vanadium from the calcification roasting pellets of vanadium titanomagnetite. *J. Mater. Res. Technol.* 23, 778–790.
- Wang, J., Wang, S., Ye, L., Li, M., Yang, L., Luo, J., Wang, X., Zhang, Z., 2022. New calcification roasting-sulfuric acid leaching: A zero-discharge, cleaner-sustainable and multi-value-added products route of vanadium. *J. Clean. Prod.* 379, Part 2, 134689.
- Wang, F., Zhang, Y., Huang, J., Liu, T., Wang, Y., Yang, X., Zhao, J., 2013. Mechanisms of acid-leaching reagent calcium fluoride in the extracting vanadium processes from stone coal. *Rare Met.* 32, 57–62.
- Wu, Y., Dai, C., Nie, Y., Tian, X., Yang, C., 2023. Effect of morphology especially leaf-like morphology on surface Fe^{2+} content of $\alpha\text{-Fe}_2\text{O}_3$ in photo-assisted fenton-like degradation of organic contaminants. *Colloid. Surface. A* 663, 131116.
- Wu, W., Wang, C., Bao, W., Li, H., 2018. Selective reduction leaching of vanadium and iron by oxalic acid from spent $\text{V}_2\text{O}_5\text{-WO}_3/\text{TiO}_2$ catalyst. *Hydrometall.* 179, 52–59.
- Xu, Y., Xia, H., Zhang, Q., Jiang, G., Zhang, L., Xin, C., Cai, W., 2023. Ultrasonic enhanced hydrazine sulfate acid leaching of low-grade germanium dust. *Appl. Energ.* 332, 120485.
- Yan, S., Sun, C., Zhou, T., Gao, R., Xie, H., 2021. Ultrasonic-assisted leaching of valuable metals from spent lithium-ion batteries using organic additives. *Sep. Purif. Technol.* 257, 117930.
- Zhang, Y., Bao, S., Liu, T., Chen, T., Huang, J., 2011. The technology of extracting vanadium from stone coal in China: History, current status and future prospects. *Hydrometall.* 109 (1–2), 116–124.